colorants

MDPI

Article

Diphenyl-Furanones and Diphenyl-Oxopyrrole Derivatives: From Analytical Reagents for Amino Groups to New Fluorochromes for Cytochemical Staining of Chromatin DNA and Chromosomes: Proposal for Intercalative Binding and Fluorescence Mechanism

Juan C. Stockert [1,2,*], Silvina A. Romero [1,3], Marcelo N. Felix-Pozzi [4] and Alfonso Blázquez-Castro [5]

1 Facultad de Medicina, Instituto de Oncología "Angel H. Roffo", Area Investigación, Universidad de Buenos Aires, Avda. San Martin 5481, Buenos Aires C1417DTB, Argentina; sromero@fvet.uba.ar
2 Centro Integrativo de Biología y Química Aplicada, Universidad Bernardo O'Higgins, General Gana 1702, Santiago 8370854, Chile
3 Cátedra de Virología Animal, Facultad de Ciencias Veterinarias, Universidad de Buenos Aires, Chorroarin 280, Bueno Aires C1427CWO, Argentina
4 Departamento de Micro y Nanotecnología, Instituto de Nanociencias y Nanotecnología, Centro Atómico Constituyentes, Comisión Nacional de Energía Atómica, Buenos Aires B1650LWP, Argentina; marcelofelixpozzi@cnea.gov.ar
5 Departamento de Biología, Universidad Autónoma de Madrid, c/Darwin 2, 28049 Madrid, Spain; alfonso.blazquez@uam.es
* Correspondence: jcstockert@institutoroffo.uba.ar

check for updates

Citation: Stockert, J.C.; Romero, S.A.; Felix-Pozzi, M.N.; Blázquez-Castro, A. Diphenyl-Furanones and Diphenyl-Oxopyrrole Derivatives: From Analytical Reagents for Amino Groups to New Fluorochromes for Cytochemical Staining of Chromatin DNA and Chromosomes: Proposal for Intercalative Binding and Fluorescence Mechanism. *Colorants* **2023**, *2*, 245–263. https://doi.org/10.3390/colorants2020016

Academic Editor: Julien Massue

Received: 9 February 2023
Revised: 19 April 2023
Accepted: 4 May 2023
Published: 15 May 2023

Copyright: © 2023 by the authors. Licensee MDPI, Basel, Switzerland. This article is an open access article distributed under the terms and conditions of the Creative Commons Attribution (CC BY) license (https://creativecommons.org/licenses/by/4.0/).

Abstract: Diaryl-furanones are specific analytical reagents for the biochemical detection of primary amines by fluorescence techniques. Well-known reagents are fluorescamine (Fluram) and 2-methoxy-2,4-diphenyl-3(2H)-furanone (MDPF), yielding fluorescent products with λem at 480–490 nm. Although the reaction products claim to be pyrrolinones, recent studies show that they are really 3-oxopyrrole (pyrrolone) derivatives. Both reagents have been used for the cytochemical demonstration of primary amines. In this work, we have applied the fluorescent products of MDPF with amines (n-butylamine, BA; glucosamine, GA; and spermine, Sp), which showed interesting fluorescence reactions with chromatin DNA. 2,4-diphenyl-3-oxopyrrole products (diPOPy) can be easily synthesized according to well-known procedures, by mixing solutions of MDPF in acetone with water at pH 9 containing the amino compounds. DiPOPy derivatives of BA, GA, and Sp were used for spectroscopic, microscopic, and molecular modeling studies, showing a bright and selective blue–green fluorescence on DNA substrates, mainly chromatin, kinetoplast DNA, and stretched chromatin fibers. The cationic diPOPy fluorophore is planar, with a high partial positive charge in the N atom, and suitable for intercalative binding to DNA. A mechanism of fluorescamine fluorescence due to an inner-salt isomeric form is proposed, and an astonishing correlation between adenine–thymine-rich centromeric heterochromatin in mouse metaphase chromosomes after reaction of the fluorescamine reagent with protein amino groups is also discussed.

Keywords: DNA staining; fluorescamine; fluorescence staining; fluorochromes; MDPF; molecular modeling; oxopyrrole derivatives; staining mechanisms

1. Introduction

It is well known that the non-fluorescent furanone reagents fluorescamine (4-phenylspiro-(furan-2-(3H)-1′-phthalan)-3,3′-dione) and MDPF (2-methoxy-2,4-diphenyl-3(2H)-furanone) do react directly and selectively with primary amines (R-NH_2) in aqueous media at alkaline pH to yield highly fluorescent products [1–5]. As fluorogenic reagents for amino

groups, fluorescamine and MDPF have found wide applications in analytical biochemistry using electrophoresis, as well as liquid and thin-layer chromatography [6–12]. They have also been used for fluorescent labeling of proteins [13–19], as reagents for modified nucleosides [20,21], and as probes for cell membranes [22,23].

Regarding fluorescence microscopy, the fluorogenic reaction with fluorescamine and MDPF also has histochemical applications for the visualization of amino groups in cells and tissues [24–29]. Interestingly enough, these furanone reagents have been proposed for the early detection of tumor cells [30–33]. It must be noted that fluorescamine- and MDPF-amino derivatives were originally formulated as 2-hydroxy-pyrrolinones [2,13,34,35] (Figure 1B,B′).

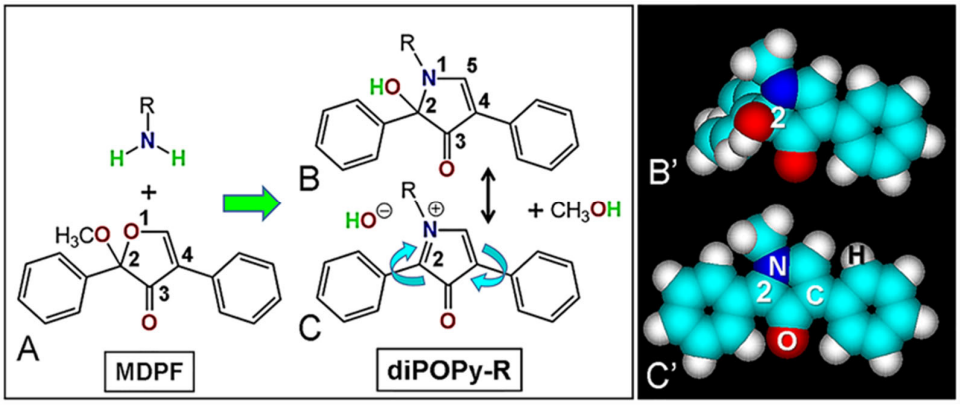

Figure 1. (**A**) Chemical reaction of MDPF with a primary amine, showing the atom numbering of the furanone. (**B**) Pyrrolinone product (2-hydroxy-3-oxopyrrole), corresponding to the non-fluorescent pseudobase at alkaline pH. (**C**) Fluorescent pyrrolone derivative (2,4-diphenyl-3-oxopyrrole, diPOPy-R) at neutral or acid pH (after replacing the hydroxyl by a stronger anion), showing the positive quaternary N, and rotation freedom of phenyl rings (curved arrows). The C2 atom is tetragonal in (**B**) and conjugated trigonal in (**C**). (**B′**,**C′**) Atomic volume models of the corresponding structures from the left, showing the different geometry of the C2 atoms (PM3 energy minimization converged at E = 0.1 kcal/(Å mol).

From these early studies and throughout the literature, 2-hydroxy-pyrrolinones have been customarily accepted as the fluorescent products of fluorescamine and MDPF with primary amines. However, for non-planar molecules, such as 2-hydroxy-pyrrolinones, the long absorption (370–380 nm) and emission (480–490 nm) wavelengths they actually show are quite unexpected features [36]. In fact, the occurrence of a tetrahedral C2 atom disrupts the conjugation of the three ring systems, thus avoiding the formation of a coplanar fluorophore, necessary for such long absorption and emission wavelengths. Therefore, the 2-hydroxy-pyrrolinone (Figure 1B,B′) just corresponds to the pseudobase of the true fluorophore, which accordingly is a coplanar, full conjugated and cationic 2,4-diphenyl-3-oxopyrrole (diPOPy, Figure 1C,C′) [37–39].

At present, previously formed fluorescent fluorescamine and MDPF products in vitro have been scarcely used as direct fluorochromes [36]. However, considering that diPOPy and the fluorescamine derivative (2-benzoic-4-phenyl-3-oxopyrrole, BzPOPy) are strongly fluorescent [13,28,29], and presuming an expected affinity of the cationic MDPF derivatives for polyanionic substrates, these derivatives could be used for staining fixed cells. Indeed, when these products were applied to fixed cells, a striking fluorescence of chromatin DNA was observed. Although a similar fluorescence is also expected to occur with other polyanionic substrates (e.g., RNA, acid glycosaminoglycans, etc.), only the selective reaction of diaryl-POPy dyes with DNA will be emphasized in the present work. An intercalative binding mode and a fluorescence mechanism for fluorescamine reaction products are also proposed and discussed here.

2. Materials and Methods

2-Methoxy 2,4-diphenyl 3(2H)-furanone (MDPF, >98% purity) was purchased from Fluka (Buchs, Switzerland). Amino compounds (n-butylamine (BA), dopamine HCl (DA), benzylamine, α-D-glucosamine HCl (GA), and spermine 4HCl (Sp)), as well as remaining reagents were purchased from Merck-Sigma-Aldrich (Darmstadt, Germany). Amino derivatives from MDPF were prepared from the amino compounds BA, GA, and Sp using well-known synthetic procedures [2,7,13,29,38], yielding the corresponding 2,4-diphenyl-3-oxopyrrole products diPOPy-B, diPOPy-G, and bis-diPOPy-Sp, respectively (Figure 2). Other amines were found difficult to use: benzylamine was practically insoluble in water, and blackening of dopamine by autopolymerization [40] hindered the fluorescence of the reaction product, so no further studies were performed with these amines.

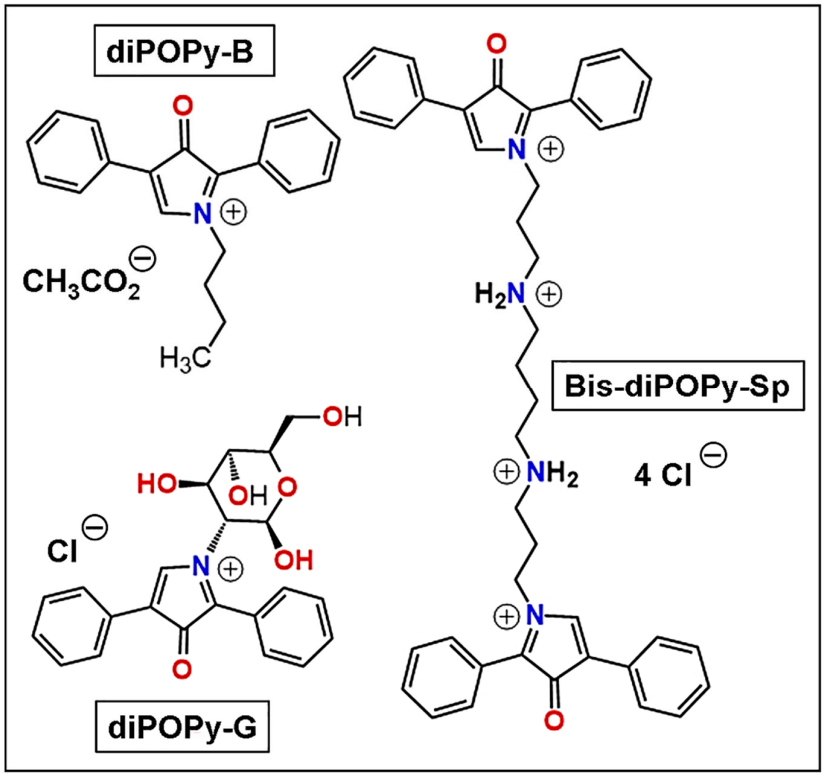

Figure 2. Chemical structure of the 2,4-diphenyl-3-oxopyrrole fluorophores used in this work: diPOPy-B, diPOPy-G, and bis-diPOPy-Sp, showing formal distribution of double bonds, positive charges, and counter ions. The number of atoms in the linker of bis-diPOPy-Sp is 12.

The fluorescent reaction products were formed directly by mixing 1:4 (v/v) a solution of MDPF (2 mg/mL in acetone) with distilled water adjusted to pH 9 containing the solid amino compounds (GA, Sp, 1 mg/mL) or a 10% solution of BA. After standing at room temperature (RT) for 5 min, the final solution was adjusted to pH 7 and either diluted 1:10 (v/v) with distilled water or allowed to dry at 40 °C. Values of pH were adjusted to 9 or 7 using sodium bicarbonate or 2.5% acetic acid, respectively. Only primary amines react with furanone reagents, giving stable fluorescent products [2–4,7,21,38]. In addition, as rapid degradation products of the reagents occur in aqueous solutions, yielding non-fluorescent 2-hydroxy-furanones [1,13,35], no other compounds are formed during the simple synthetic procedure described here.

As model microscopic structures, erythrocyte nuclei from chicken blood smears [41–43], kinetoplasts from *Trypanosoma cruzi* (*T. cruzi*) epimastigotes growing in culture [44,45], and well-orientated 30 nm chromatin fibers from stretched nuclei [46,47] were used by allowing a precise analysis of fluorescence staining reactions of chromatin DNA.

For staining procedures, samples of chicken blood and mouse spleen smears, as well as smears of *T. cruzi* epimastigotes (12×10^6 cells/mL) growing at 27 °C, were fixed in methanol for 2 min and stained with a 20 µg/mL solution of diPOPy-B or bis-diPOPy-Sp in distilled water for 5 min, washed in distilled water, air-dried, and mounted in DePeX. Before staining, some smears were subjected to DNA extraction by using DNase I (Sigma, 0.5 mg/mL in 1 mM $MgCl_2$ at 37 °C for 2 h) or 5% trichloroacetic acid (TCA, at boiling temperature for 20 min). After staining, some chicken blood and mouse spleen smears were also washed for 30 min with either aqueous 2 M NaCl solution, 4 M urea, or a saturated aqueous solution of caffeine or ortho-phenanthroline, which are known competitive assays for revealing dye binding by electrostatic forces, H-bonding, or hydrophobic interactions, respectively [36,48].

On the other hand, from a historical perspective and for comparative purposes, the microscopic visualization of amino groups from basic proteins is also presented here using the pristine analytical reagent fluorescamine. As model microscopic structures, horse eosinophils containing basic proteins are very suitable cells on account of the large size of their highly acidophilic granules, allowing a precise analysis of fluorescence reactions [29,49,50]. In this case, a solution of fluorescamine (0.5 mL of a 0.5 mg/mL solution in acetone) was added to methanol-fixed smears of horse blood previously covered with 0.5 mL of borate buffer at pH 9 [28]. After treatment for 5 min at RT, smears were washed in distilled water, air-dried, and mounted in DePeX.

Microscopic observation and photography were performed using an Olympus BX-61 epifluorescence photomicroscope (Hamburg, Germany) equipped with an HBO 100-W mercury lamp and the ultraviolet (UV, 365 nm) exciting filter. Images were captured with an Olympus DP50 CCD camera and processed using Adobe Photoshop 6.0 (San José, CA, USA) and PowerPoint 2000 (Microsoft, Redmont, WA, USA) software. Unstained smears were previously analyzed for autofluorescence, which in all cases was negligible.

Spectroscopic studies on diPOPy derivatives (10–20 µg/mL in distilled water at pH 7) were performed using a spectrophotometer Shimadzu UV-VIS 1604, Columbia, MD, USA, and a spectrofluorometer Perkin-Elmer 650-10S (Chicago, IL, USA) equipped with a 150-W xenon lamp, two grating monochromators, the Hamamatsu R372F detector (wavelength range: 220–730 nm), and excitation at 360 nm. When used in the normal mode, emission spectra that are corrected for variation in the excitation intensity are obtained. Because of its negligible contribution, the Raman scattering of solvents was not subtracted from emission spectra.

Molecular parameters were studied by simple inspection of chemical structures such as the conjugated bond number (CBN, for the overall size of the conjugated system), and calculated or measured molecular size (width/length, W/L values) [51]. Molecular modeling studies on protonated diPOPy (diPOPy-H), diPOPy-G, and bis-diPOPy-Sp intercalated into an AT-DNA tetramer, as well as fluorescamine and its reaction products with amino groups (BzPOPy), were carried out using the HyperChem v7 and v8.0.10 software (Hypercube, Inc., Gainesville, USA). As performed in previous molecular modeling studies [52,53], geometry optimization was achieved with the MM+ routine, followed by energy minimization by either the semi-empirical PM3 method (Polak–Ribière conjugate gradient) converged at 1, 0.5, 0.2, or 0.1 kcal/(Å mol), or using the extended Hückel method.

3. Results

3.1. DiPOPy Fluorochromes from MDPF

The aspects of freshly made GA and diPOPy-G solutions (20 µg/mL in distilled water adjusted to pH 7) either under day light illumination or 420 nm excitation are shown in Figure 3A,B, which clearly reveal a light yellow absorption color and the bright blue–green fluorescence of diPOPy-G.

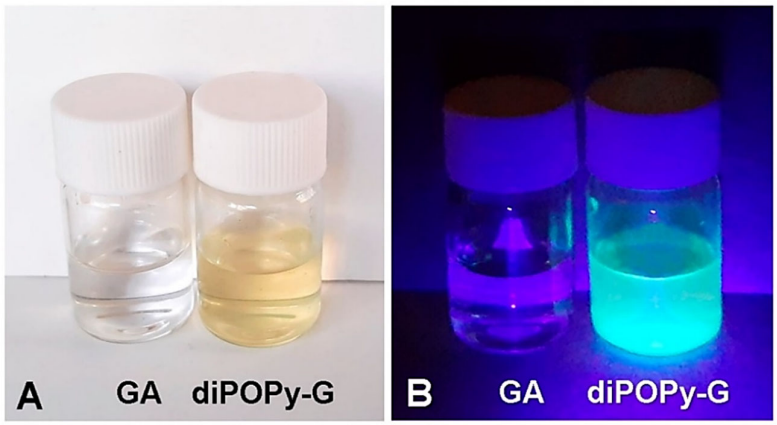

Figure 3. (**A**) Samples of GA alone and diPOPy-G (20 µg/mL in distilled water at pH 7) under day light illumination. (**B**) The same samples under 420 nm exciting light from a blue–violet laser pointer. Observe the light yellow absorption color and the bright blue–green emission of diPOPy-G.

Identical absorption and fluorescence colors are also found in diPOPy-B and bis-diPOPy-Sp. Spectroscopic studies of diPOPy-B, diPOPy-G, and bis-diPOPy-Sp revealed absorption and emission maxima at 385 and 487 nm, respectively. Absorption and emission spectra of diPOPy-B (10 µg/mL in distilled water at pH 7) are shown in Figure 4. At neutral pH, all solutions were stable, and no spectral changes were found at mild alkaline or acid pH values. In the presence of 45% glycerol, 60% sucrose, and 40% dextran 60 in water, samples showed an emission peak about twice higher than that of aqueous solutions (not shown), which indicates the dependence of the fluorescence intensity on the viscosity of the solvent. Another solvent feature that modulates fluorescence wavelength red-shift is its dielectric constant. The dielectric constant is a measure of how efficiently the solvent responds to the altered electronic distribution of the fluorophore in the excited state. A solvent with a high dielectric constant (e.g., water) quickly reorients its dipoles to shield the altered electric field surrounding the excited molecule. This reorientation implies the use of energy that comes from the excited state. Therefore, once equilibrium is reached, which takes less than a picosecond, the available energy for photon emission is less (red-shifted) as compared with the initial energy absorbed. Solvents with high dielectric constant (polar solvents) show a more pronounced reorientation effect than solvents with a small dielectric constant (non-polar solvents). In the solid state, microcrystals of POPy derivatives also exhibited strong fluorescence under 365 nm excitation.

After staining suitable microscopical preparations with the fluorochromes diPOPy-B, diPOPy-G, and bis-diPOPy-Sp, a bright blue–green fluorescence was observed in DNA-containing structures. Methanol-fixed nuclei from chicken blood smears showed a strong and selective emission (Figure 5A,B), with some fading degree like most organic fluorochromes.

Likewise, after diPOPy staining, smears of *T. cruzi* cultures (Figure 6A), chromatin DNA of leucocyte nuclei from mouse spleen smears, as well as elongated chromatin fibers produced by stretching of spleen smears, showed a bright blue–green fluorescence. In this case, the observation of stretched chromatin fibers using bright-field illumination (Figure 6B) and polarization microscopy (Figure 6C,D) pointed out that the brighter fluorescence occurred when the analyzer filter was perpendicular to the direction of chromatin fibers, whereas a parallel orientation between them resulted in a weaker emission ($\perp > \|$). This agrees with an orthogonal position of the diPOPy fluorophore and the nucleosomal DNA axis, indicating an intercalative binding mode to DNA [46].

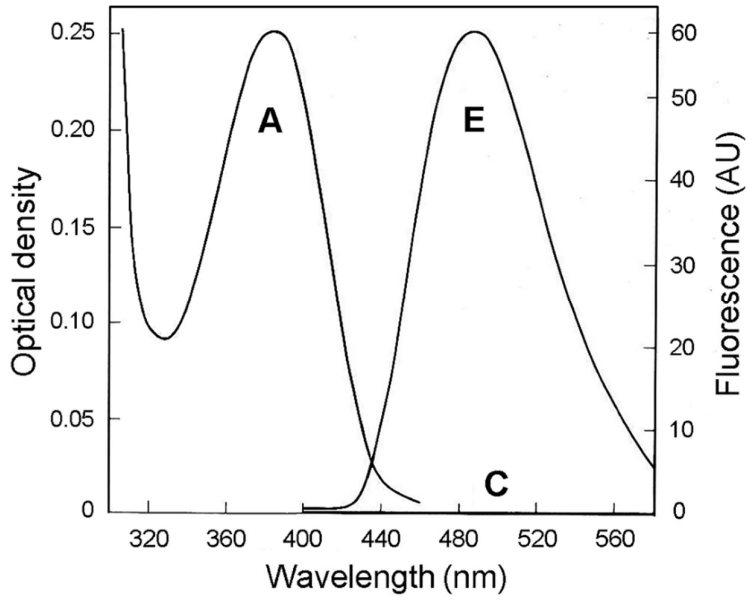

Figure 4. Normalized absorption A and emission E spectra of a 10 μg/mL solution of diPOPy-B in distilled water at pH 7. The line C corresponds to the emission of the reagent MDPF alone in the absence of BA. No emission was found for BA alone. Exciting light: 360 nm.

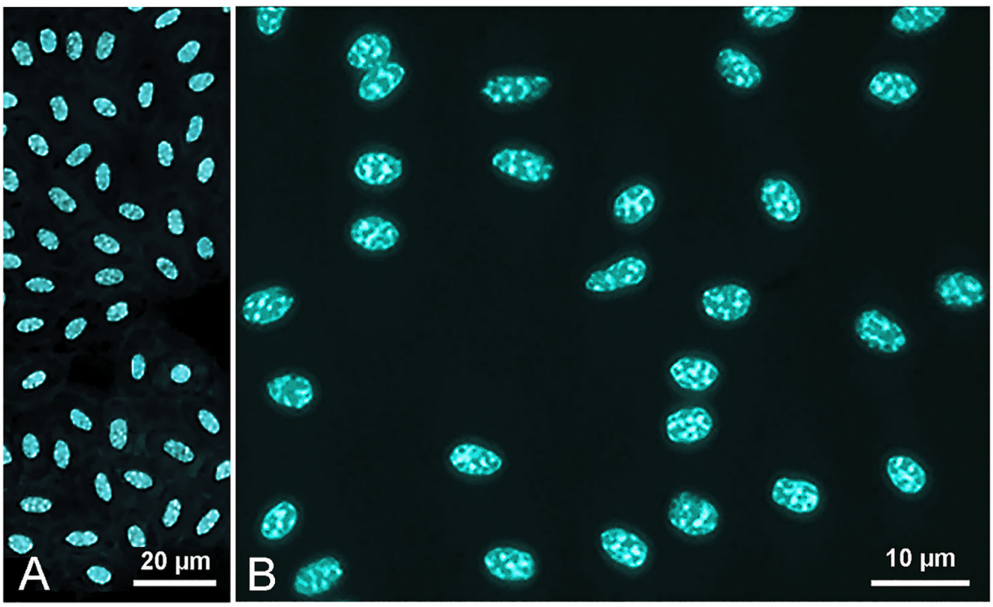

Figure 5. Fluorescence images of chicken blood smears fixed in methanol and stained with diPOPy-G (**A**) and bis-diPOPy-Sp (**B**), showing the bright and selective blue–green emission of DNA in compact heterochromatin masses from interphase erythrocyte nuclei.

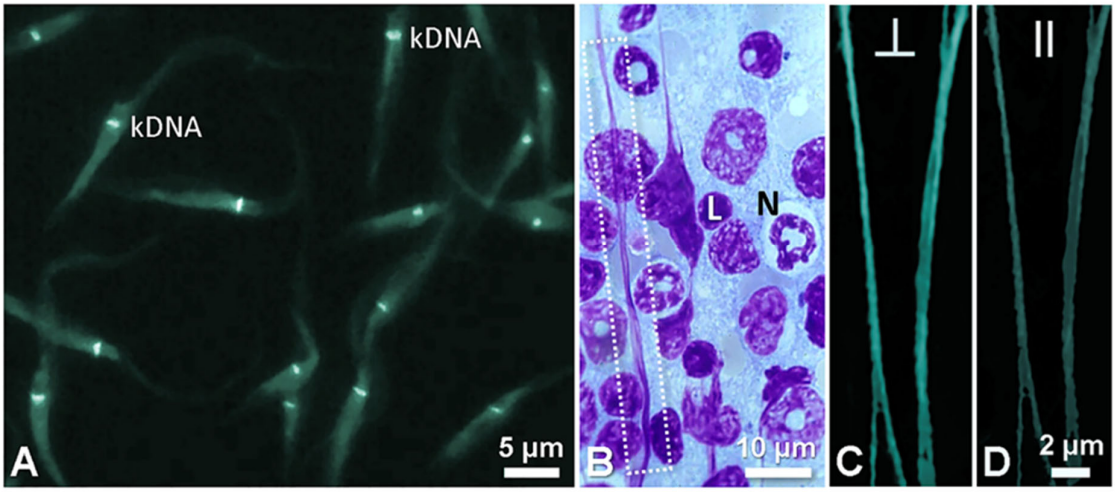

Figure 6. (**A**) Cultured *T. cruzi* epimastigotes stained with bis-diPOPy-Sp showing the blue–green fluorescence of kinetoplast DNA (kDNA, bright transverse rod in each cell). (**B**) Stretched mouse spleen smear after Giemsa staining, showing elongated nuclei containing longitudinally orientated chromatin fibers (dashed rectangle). Observe the typical magenta color of chromatin and the light blue color of basophilic cytoplasm [54]. N: neutrophil; L: lymphocyte. (**C**,**D**) Stretched chromatin fibers from a mouse spleen smear stained with diPOPy-B and observed under polarization microscopy, by using perpendicular (**C**) and parallel (**D**) positions of the analyzer filter in relation to the axis of the stretched chromatin fibers, showing emission intensity: $\perp > \parallel$, which is a typical feature of intercalating agents.

In control samples, after previous treatment of chicken blood, *T. cruzi* cultures, and mouse spleen smears with DNase and TCA, the emission induced by diPOPy-B and bis-diPOPy-Sp was negative, which indicates that DNA-containing structures are the substrate responsible for the fluorescence reaction. Washing of stained preparations with 2 M NaCl and 4 M urea solutions did not result in reduction of the fluorescence intensity, while washing in saturated aqueous solutions of caffeine or ortho-phenanthroline clearly diminished the emission, also indicating the occurrence of hydrophobic and non-ionic binding forces between fluorochromes and the DNA substrates [36,48].

Inspection of the chemical structures reveals that diPOPy is a small and planar molecule, with CBN: 20, and calculated (bonds) or measured (Å) W/L: 0.4 and 0.46, respectively, which correspond to the classical appearance of a "tea-tray" very suitable for intercalation [51]. After geometry optimization and energy minimization, molecular modeling studies showed a full conjugated aromatic structure, with a clear and differential distribution of partial charges (Figure 7A).

Regarding molecular orbitals of diPOPy-H (Figure 7B), energy levels of higher occupied and lower unoccupied molecular orbitals (HOMO-0 and LUMO + 0, respectively) are well separated (LUMO + 0 subtracted from HOMO-0 = Eg = 6.01 eV), which is related to the large Stokes shift and a blue–green emission under UV excitation. As expected, the number of nodal planes is higher for LUMO + 0 than for HOMO-0 [36,40].

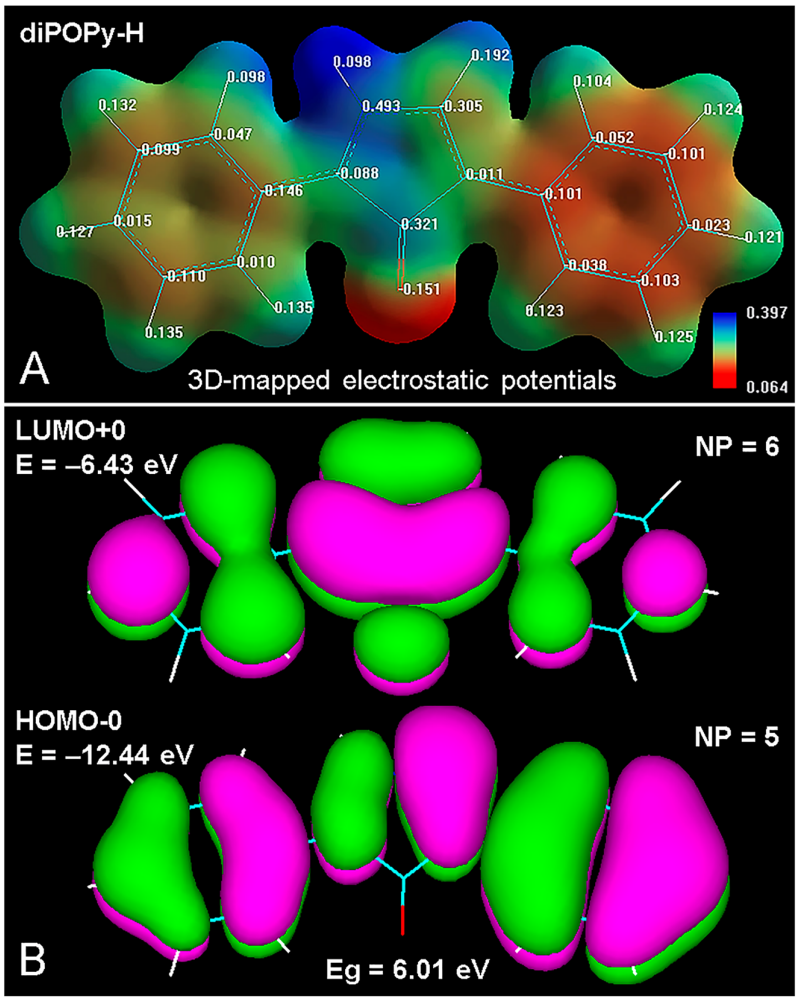

Figure 7. Molecular modeling of the protonated derivative diPOPy-H. (**A**) Partial charges (eV), and 3D plotting of electrostatic potentials (from negative to positive values: red → green → blue), using HyperChem v8.0.10 (Hypercube, Inc., Gainesville, FL, USA).and PM3 converged at E = 0.1 kcal/(Å mol). Translucent isosurface rendering (total charge density contour value: 0.02). (**B**) HOMO-0 (ground state) and LUMO + 0 (first excited state) energy levels (orbital contour value: 0.015, tilt: 15°), showing the almost symmetrical π-electron orbital lobes in different colors. NP: number of nodal planes separating different orbital lobes.

In the case of a hypothetical dye–substrate structure, molecular modeling reveals that adenine–thymine (AT)-containing nucleic acid oligomers such as tetra-(dATAT) can be bis-intercalated by bis-diPOPy-Sp, appearing as the two fluorophore rings separated by ~10.2 Å, in agreement with the "nearest neighbor exclusion principle" for intercalating agents [36,55,56]. Although there is not precise evidence for specific binding to AT base pairs, some presumptive cytological and cytogenetic data support this possibility. Figure 8 shows wire (A) and atomic volume (B) models of the bis-intercalated complex, as well as the overlapping (fused) molecular orbitals (MOs) between each dye and base pairs above and below (C), and the non-overlapping (unfused) MOs between adjacent base pairs, which abolish the in-phase π-electron conjugated stacking in these sites.

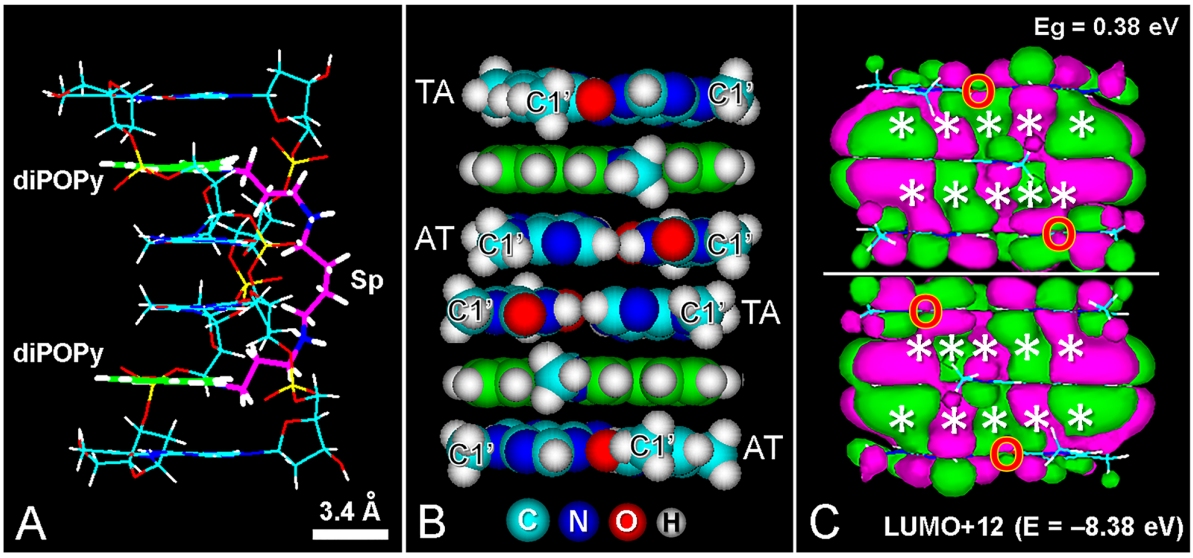

Figure 8. (**A**) Lateral view of a wire model of tetra-(dATAT) bis-intercalated by bis-diPOPy-Sp after geometry optimization with MM+ converged at E = 0.2 kcal/(Å mol). Green and violet colors represent C atoms from diPOPy and spermine (Sp), respectively. Winding angles are 36° between stacked base pairs and 18° between intercalated ones. (**B**) Atomic volume model of the same structure, with AT bases bis-intercalated by two planar fluorophores from bis-diPOPy-Sp, viewed from the minor groove. For clarity, phosphate–sugar chains and the spermine linker are not shown. C1′ atoms are represented as methyl groups. C atoms from diPOPy are green. Red oxygen atoms are O_2 from thymine. (**C**) The same molecular complex, after energy minimization (extended Hückel method for 576 orbitals) showing the 3D isosurface plotting of LUMO + 12 (E = −8.38 eV, contour: 0.001). HOMO-0: −11.63, LUMO + 0: 11.25 eV. Green and violet colors correspond to molecular orbitals with different signs (+ and −). Overlapping orbitals are indicated by asterisks. The white line is the gap lacking fused orbitals. **O**: O2 atoms from thymine.

It is worth noting that all the LUMOs at low energy levels (from +0 to +12) showed full overlapping MOs between the intercalated diPOPy and its adjacent base pairs. However, only partially or non-overlapped MOs appeared between stacked base pairs, which indicates that the intercalator corresponds to an electronically isolated monomer within the intercalation cavity.

3.2. BzPOPy Fluorochromes from Fluorescamine

Although the fluorescence mechanism of the reaction product of MDPF with amino groups at neutral pH is now well known (involving the formation of planar, full conjugated and highly fluorescent diPOPy derivatives), the mechanism allowing fluorescence of fluorescamine derivatives is not so clear. As occurs for MDPF products, at alkaline pH, the pseudobase (carbinol) of the non-planar and non-fluorescent BzPOPy product is first formed, and fluorescence only appears at neutral pH [34,38,39].

In order to illustrate the fluorescamine-induced fluorescence of amino groups in situ, the reaction was carried out on horse blood smears, which revealed the basic proteins of the eosinophil leucocyte granules [29,50] generating a strong blue–green emission (Figure 9A).

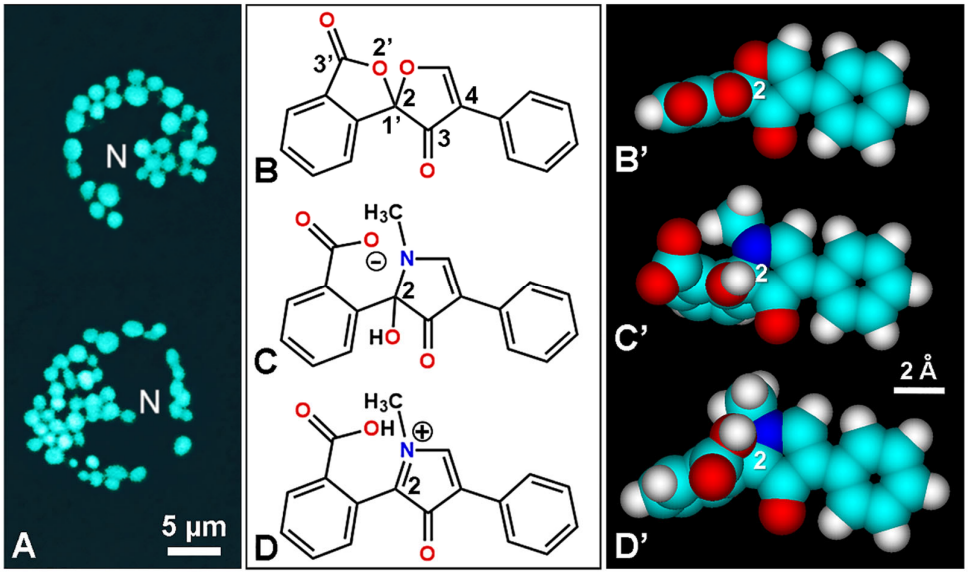

Figure 9. (**A**) Fluorescence micrograph of horse eosinophil leucocytes after staining with fluorescamine. Note the bright blue–green emission of eosinophilic granules in the cytoplasm. N: bilobed nuclei (dark volume). Fluorescence registered under UV exciting light. (**B**–**D**) Chemical structure and numbered positions of the fluorescamine lactone (**B**), the pseudobase of the reaction product with methyl-amine at alkaline pH (**C**), and the cationic product at strong acid pH with unionized carboxyl group (**D**). (**B′**–**D′**) Corresponding atomic volume models after PM3 converged at E = 0.1 kcal/(Å mol), showing the almost orthogonal geometry of the benzoic acid ring relative to the other two rings. Element colors as in Figure 1.

However, the relations between chemical structure, pH, and fluorescence features are intriguing, and no structures of the reaction product are expected to be fluorescent. Obviously, in the lactone reagent (Figure 9B,B′) there is a benzoic ring perpendicular to the other two aromatic rings. The same orthogonal geometry appears after molecular modeling of the pseudobase at alkaline pH (Figure 9C,C′), as well as in the cationic form at very low acid pH with the unionized carboxylic group (Figure 9D,D′), and thus no fluorescence should occur for these non-planar structures. Likewise, the non-charged lactone of the BzPOPy product also appears orthogonal.

Therefore, it is tempting to assume that, at about neutral pH, the quaternary N1 and carboxylate anion could equilibrate charges themselves, forming the "inner salt" (zwitterion) with a full conjugated planar geometry, which could be the true fluorescent product from the fluorescamine reaction (Figure 10). The same planar configuration of the fluorophore is found for the reaction products with arginine and lysine. The corresponding HOMO-0 and LUMO + 0 levels (not shown) are very similar to those of MDPF products. Examples of inner-salt colorants and fluorochromes (zwitterionic phenol blue, indophenol blue, merocyanine 540, Nile red, rhodols, Bodipy dyes, etc.) are also known [36,57,58].

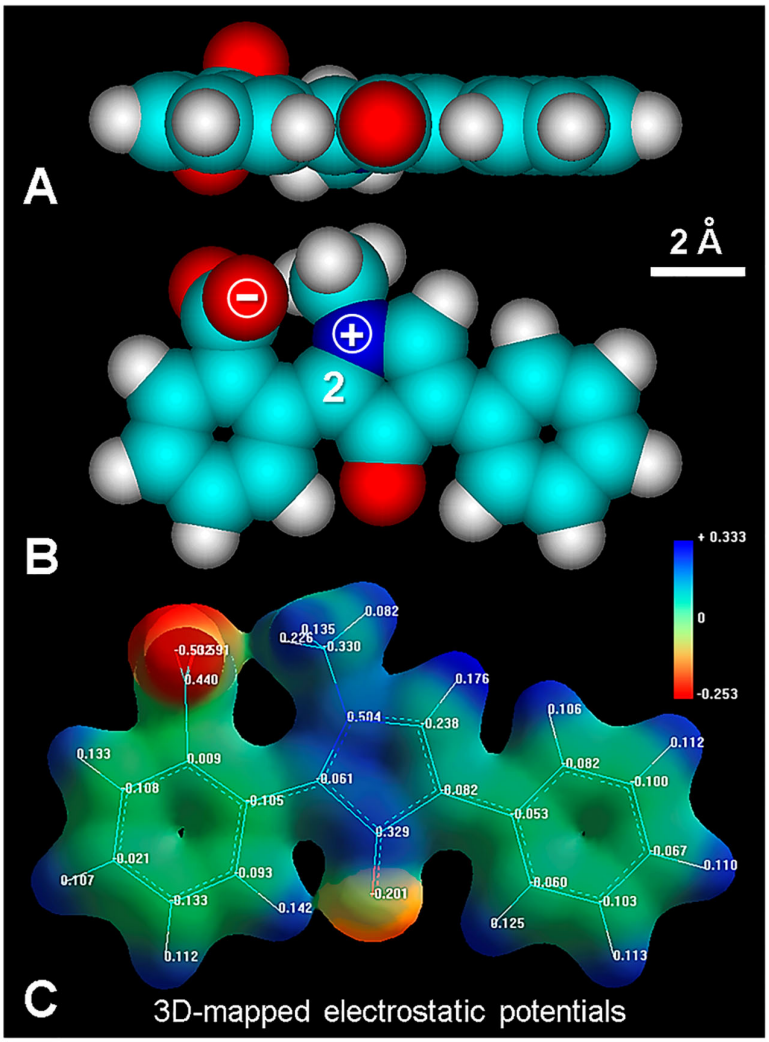

Figure 10. (**A**,**B**) Molecular modeling of the possible reaction product between fluorescamine and methyl-amine at neutral pH, showing the planar structure in lateral and frontal atomic volume views, respectively. Negative and positive signs correspond to the formal positive and negative charges of the tentative inner-salt (zwitterion) form of the planar BzPOPy fluorophore from fluorescamine. The trigonal C2 atom is indicated. Element colors as in Figure 9. (**C**) The same molecule showing partial charges (eV), and 3D plotting of electrostatic potentials (from negative to positive values: red → green → blue), using the translucent isosurface rendering (total charge density contour value: 0.03), after energy minimization with HyperChem v8.0.10 and PM3 converged at E = 0.5 kcal/(Å mol). Partial charges for the N and O atoms from the inner salt are + 0.504 and −0.591 eV, respectively.

4. Discussion

4.1. DiPOPy Derivatives as Fluorochromes

The design and development of new fluorochromes and fluorescent probes are of increasing interest in biomedical fields, and they have been extensively reviewed [36,44,51,55,59,60]. A few examples are new cationic fluorochromes highly selective for microscopical visualization of DNA, containing chemical groups such as isoquinoline [61] and β-carboline [41] alkaloids, benzothiazole [62], phenyl-pyrrole-quinolinium [63], quinolinium-benzoxazole and -benzothiazole [64], naphthalimide [42], phenyl-diamidine [45], phenyloxazole scintillators [65,66], benzimidazole-sulfonamide [67], etc.

Considering the small size, planar structure, and cationic status of the POPy fluorophore, an intercalative binding mode between base pairs of a DNA duplex is expected to occur, as well as bis-intercalation in the case of bis-diPOPy-Sp. Polarized fluorescence is a suitable microscopical tool to analyze the orientation of fluorochromes in both well-

orientated DNA and chromatin fibers [46,51,68]. An intercalative binding mode is expected to occur when the polarization and fiber axis orientation are perpendicular ($\perp > \|$).

There are still no data about the possible preference of intercalation related to AT or GC. It is known that daunomycin and berberine allow the visualization of AT-rich chromosome regions (Q banding) by fluorescence microscopy [36,55,61,69]. Likewise, quinacrine and quinacrine mustard fluoresce brighter in AT-rich regions, and it is generally accepted that Q-negative bands are produced by fluorescence quenching by guanine [70–73].

On the other hand, abundant $(dA)_{4\text{-}6} \bullet (dT)_{4\text{-}6}$ sequences are present in the kDNA [74]. Minicircles of kDNA contain repeated short $(dA)_{4\text{-}6} \bullet (dT)_{4\text{-}6}$ tracks alternating with normal DNA sequences, which generates the curved DNA structure typical of kDNA minicircles [75]. Likewise, the pericentromeric heterochromatin DNA regions of mouse chromosomes (C-bands) are AT-rich (approximately 69% AT), appearing composed of a highly repetitive 230–240 base pair unit [76], which contains the EcoRI GAATTC restriction site and numerous consecutive $(dA)_{4\text{-}6} \bullet (dT)_{4\text{-}6}$ tracts [77]. Therefore, due to the high AT content in kDNA and C-bands of mouse chromosomes, they can be used as a suitable test model to analyze the selectivity of fluorochrome binding at the microscopical level.

In keeping with this, the selective fluorescence of interphase heterochromatin from chromatin DNA (Figure 5) and kDNA (Figure 6A) could be attributed to some preference for diPOPy to bind to AT-rich regions. According to the equation E (eV) = 1239.847/λ(nm), the energy gap (Eg) between the ground singlet $S_{0.0}$ and the first excited singlet $S_{1.0}$ of diPOPy-B corresponds to the cross (iso-absorptive/emissive) point at 435.5 nm and 2.846 eV. From these values, 2.545 eV for the 487 nm blue–green emission is obtained.

Regarding molecular modeling of POPy derivatives, simple aliphatic residues (e.g., diPOPy-B) have a rather linear structure. In the case of diPOPy-G, the C1–N1 bond is able to rotate; the hexose ring of the bulky glucosyl residue and the planar diPOPy ring are almost perpendicular. The possible intercalative binding of diPOPy-G could be accomplished with the glucosyl residue located in the minor groove, as occurs with the phenyl group of ethidium bromide and the daunosamine group of daunomycin [56,78].

4.2. Bis-Intercalative Binding

Bis-intercalation occurs when two aromatic chromophores (fluorophores) separated by a flexible or rigid linker of ~10.2 Å become inserted into a DNA duplex, which is the case for some antibiotics and synthetic dyes and drugs [36,56,60]. In addition, several synthetic bis-intercalators are well-known fluorescent colorants, and they are used in microscopy and cytofluorimetry to detect and quantify DNA. Examples are 9-amino-acridine fluorophores attached by linkers with different structures and sizes [79]. The synthetic bis-intercalating fluorochromes TOTO-1 and YOYO-1 show high affinity for DNA and have wide applications for DNA imaging [64,69,80,81] due to their large increase of emission after DNA intercalation, which avoids the rotational energy decay of excited fluorophores with torsional freedom [36,82,83].

Most known bis-intercalating DNA fluorochromes (ethidium homodimer-1, TOTO-1, and YOYO-1), contain a positively charged and flexible aliphatic bridge between the intercalating cyanines. Although the use of a spermine linker has been applied for a 9-amino-acridine bis-intercalator [79], as far as we know, the spermine bridge appears as a rather overlooked linker for bis-intercalating DNA fluorochromes. The fluorogenic reaction of spermine with fluorescamine has been previously described [1,34]. Spermine is a tetracation at physiological pH and it appears as a flexible aliphatic linker that is very suitable to bridge two terminal POPy intercalators, as occurs in the case of bis-diPOPy-Sp (see Figures 2 and 8).

Apart from fluorescent labeling, bis-intercalating drugs containing suitable chromophores have biomedical applications. The biological activity and therapeutic action of DNA intercalating and bis-intercalating drugs have been reviewed [84,85]. Quinoxaline antibiotics echinomycin and triostin A bis-intercalate their quinoxaline rings into DNA and recognize GC/CG base pairs [86]. Likewise, the antitumor antibiotic carzinophilin A

bis-intercalates two naphthalene rings into DNA, inducing interstrand cross-linking by means of its two alkylating aziridines [87].

Other antitumoral bis-intercalators are the quinoline luzopeptin A, thiocoraline, and SW-163C compounds [85,88,89]. Two phenazine rings can be bound by an aliphatic chain, thus forming a synthetic bis-intercalating anti-cancer drug. This is the case of XR5944 (MLN944), which induces inhibition of DNA topoisomerases I and II [90–93]. Likewise, the indeno-isoquinoline bis-intercalator NSC727357 is a topoisomerase inhibitor with antitumor activity [94]. Ditercalinium is another DNA bis-intercalator with anticancer activity and intriguing repair-inducing properties [95].

Two 3-amino-naphthalimide fluorophores [42] linked by a spermine bridge can generate a bis-intercalating naphthalimide, which induces bright emission in chromatin DNA [36]. Bis-naphthalimides are also antitumor agents [96]. Regarding the possible intercalative and bis-intercalative binding mode of diPOPy fluorochromes, their physiological consequence could induce an inhibition of the replication and transcription activity of DNA, suggesting interesting pharmacological applications of these fluorescent colorants in cancer chemotherapy (e.g., [97]).

4.3. Fluorescence Mechanisms of Fluorescamine Products

As the mechanistic knowledge of histochemical reactions is a relevant issue that must be considered to avoid misleading interpretations [39], in this work we describe some microscopic and spectroscopic characteristics of MDPF fluorogenic reactions and show that, although the pseudobase is originally formed at alkaline pH, a full conjugated, cationic and planar molecule seems to be the true fluorescent product [38].

In the case of fluorescamine, a loss of fluorescence occurs at acid pH (<~4) by formation of the non-planar lactone [34], in agreement with the ionization constant of benzoic acid (pKa: 4.2). In this low-pH structure, the C2 atom becomes tetrahedral and the BzPOPy product remains non-planar. On loss of the more acidic carboxylic proton, the molecule can also exist as the free carboxylate ion, which in turn can form an inner salt (zwitterion) with the quaternary N1 atom. This polar, water-soluble form would be an equivalent of the water-insoluble lactone form, which when dissolved in organic solvents does not have color or fluorescence. It is logical to assume that the inner salt is then responsible for the emission of the fluorescamine product at pH ~7, when no more pseudobase is present, and the BzPOPy inner salt becomes planar and fluorescent again (see Figure 9A).

An example of cytochemical visualization of protein amino groups by staining mouse metaphase chromosomes with fluorescamine is reproduced in Figure 11 [28]. In this case, the strong and mild fluorescence of C and Q/G bands, respectively, are very apparent, and the close correspondence between the position of these chromosome bands and the emission of the fluorescamine–amino group product is astonishing.

It is worth noting that both lysine and arginine are revealed by the fluorescamine fluorescence reaction [1,34], yielding the BzPOPy products (Figure 12). Interestingly, arginine binds either to phosphate groups across the minor groove [78,98–100] or major groove [101,102], or to AT-rich sequences within a narrowed minor groove [103], whereas lysine also binds to phosphate groups [102].

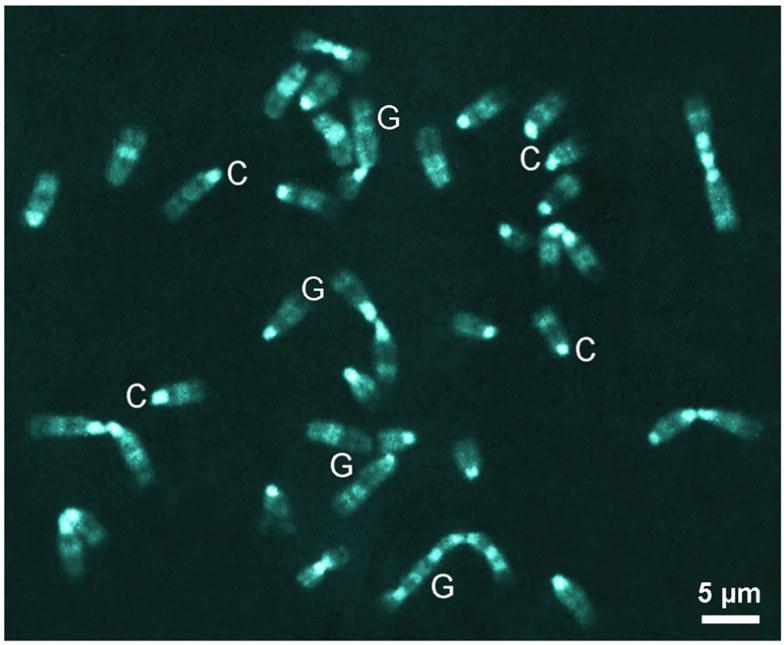

Figure 11. Metaphase chromosomes from a cultured mouse L-929 cell stained with fluorescamine, washed in tap water and mounted in a McIlvaine buffer (pH 7) glycerol–$MgCl_2$ mounting mixture, showing the strongly fluorescent C-bands (AT-rich pericentromeric heterochromatin (C)), and also considerable emission of Q/G-bands (G) (adapted with permission from Ref. [28] 2012, Copyright Clearance Center, Marketplace Chicago, IL 60673-1291).

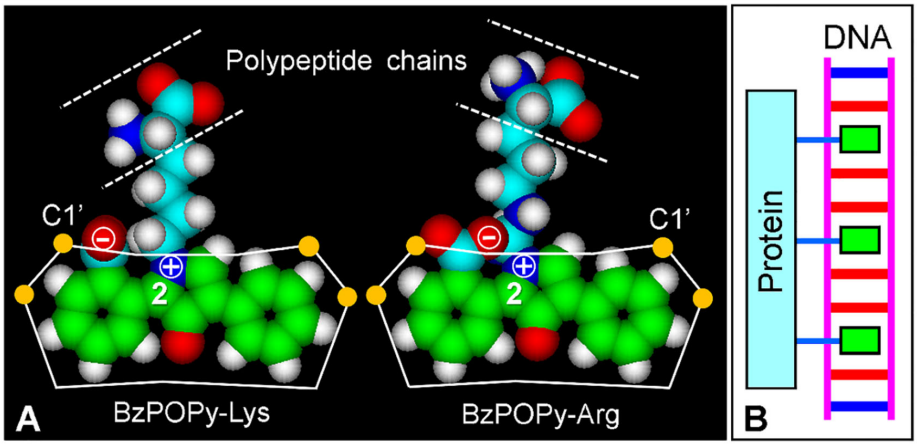

Figure 12. (**A**) Frontal views of the molecular structure (atom volume) of the fluorescent reaction products BzPOPy-Lys (total charge: 0) and BzPOPy-Arg (total charge: +1 due to the guanidino group) from fluorescamine and the respective amino acids. Molecular modeling with PM3 converged at E = 1 kcal/(Å mol). Reaction products show formal positive and negative charges forming the inner salt, and trigonal C2 atoms (2) in the planar BzPOPy fluorophores. Polypeptide chains with Lys and Arg are marked (dashed lines). Partial charges of N and O atoms are +0.51 and −0.55 eV for Lys, and +0.42 and −0.31 eV for Arg, respectively. The overlap between stacked AT base pairs (unwinding angle: 18°) in the intercalating cavity (white lines) and the intercalated fluorophores with C atoms in green are shown. Deoxyribose C1′ atoms are yellow circles. Element colors as in Figure 1. (**B**) Schematic view of the intercalative binding of BzPOPy-Lys and BzPOPy-Arg from basic proteins attached to DNA. Red and blue base pairs are AT and GC, respectively. Violet lines are the sugar-phosphate chain. Green rectangles are the intercalated fluorophores.

As the fluorescamine reactions that reveals protein amino groups from arginine and lysine residues near to the negatively charged floor of the DNA minor groove [104] colocalize with AT-rich chromosome regions, it is tempting to speculate that DNA intercalation of BzPOPy takes place precisely within these regions. The observed more intense fluorescence can be due to the rigid intercalative binding of the planar inner-salt fluorophore. As the phenyl and benzoic rings of BzPOPy can rotate lightly, a close fitting of the high propeller-twisted $(dA)_n \bullet (dT)_n$ regions [105] with the intercalated fluorophore would occur. The flexible bridge of five and six atoms (lysine and arginine, respectively) between the fluorophore and the polypeptide chain could also provide the approach needed for suitable DNA intercalation (Figure 12A). A schematic representation of the proposed intercalation of BzPOPy-Lys and BzPOPy-Arg from labeled proteins into DNA containing dA_6dT_6 sequences is shown in Figure 12B.

The absence of chromatin fluorescence after the fluorescamine reaction (see Figure 9A) deserves some comments. It is possible that, after methanol fixation, amino groups from nuclear cationic proteins could remain attached to DNA and are non-available to react with fluorescamine. The usual cytogenetic protocol using hypotonic treatment, fixation with methanol–acetic acid, and cell spreading could be relevant to disorganize the chromatin structure, improving the substrate reactivity and banding pattern. In keeping with this, fluorescamine fluorescence was found to be dependent on the fixative, chromatin, and chromosomes showing high emission after use of acetic-acid-containing fixatives [26]. A rigid intercalative binding mode will also increase the emission of tagged structures.

5. Conclusions

In this work, we show that planar and cationic diPOPy or neutral BzPOPy products are strongly fluorescent dyes that can bind selectively to chromatin DNA, likely by intercalation into AT-rich chromosome regions. Likewise, a planar inner-salt BzPOPy fluorophore is proposed for the reaction product of protein amino groups with fluorescamine. Interestingly, there is no formal charge in this type of compound, and thus no binding with anionic substrates (only based on ionic forces) should occur. These fluorescence mechanisms are supported by molecular properties and microscopical evidence, which are shared with well-known DNA intercalators. Although further studies are obviously necessary to ascertain better the affinity and selectivity for a wider range of cell and tissue substrates, it is tempting to assume that, like known intercalating and bis-intercalating antibiotics and synthetic drugs, these new diaryl-POPy derivatives could well be used in DNA cytochemistry and would also be of potential pharmacological value in cancer chemotherapy.

Author Contributions: Conceptualization, J.C.S.; methodology, A.B.-C.; software, J.C.S. and M.N.F.-P.; investigation, S.A.R.; writing—original draft preparation, J.C.S. and A.B.-C.; writing—review and editing, A.B.-C.; supervision, J.C.S. All authors have read and agreed to the published version of the manuscript.

Funding: This research received no external funding.

Acknowledgments: We thank J.L. Bella, M.M. Blanco, A.G. Casas, L.L. Colombo, R.W. Horobin, A. Stockert, and A. Urtreger for valuable collaboration, stimulating discussions, and critical reading of the manuscript.

Conflicts of Interest: The authors declare no conflict of interest.

References

1. Udenfriend, S.; Stein, S.; Böhlen, P.; Dairman, W.; Leimgruber, W.; Weigele, M. Fluorescamine: A reagent for assay of amino acids, peptides, proteins and primary amines in the picomole range. *Science* **1972**, *178*, 871–872. [CrossRef] [PubMed]
2. Weigele, M.; De Bernardo, S.L.; Tengi, J.P.; Leimgruber, W. A novel reagent for the fluorometric assay of primary amines. *J. Am. Chem. Soc.* **1972**, *94*, 5927–5928. [CrossRef]
3. Böhlen, P.; Stein, S.; Dairman, W.; Udenfriend, S. Fluorometric assay of proteins in the nanogram range. *Arch. Biochem. Biophys.* **1973**, *155*, 213–220. [CrossRef]
4. Lai, C.Y. Detection of peptides by fluorescent methods. *Meth. Enzymol.* **1977**, *47*, 236–243.

5. Toome, V.; Wegrzynski, B. Application of MDPF and fluorescamine. XV. Chiroptical properties of MDPF condensation compounds with dipeptides in situ. *Biochem. Biophys. Res. Commun.* **1983**, *114*, 433–439. [CrossRef] [PubMed]
6. Felix, A.M.; Jimenez, M.H. Usage of fluorescamine as a spray reagent for thin-layer chromatography. *J. Chromatogr.* **1974**, *89*, 361–364. [CrossRef]
7. Samejima, K. Separation of fluorescamine derivatives of aliphatic diamines and polyamines by high-speed liquid chromatography. *J. Chromatogr.* **1974**, *96*, 250–254. [CrossRef]
8. Tata, S.J.; Moir, G.F.J. Fluorescamine as a reagent for location of proteins after electrophoresis in starch gel or on paper. *Anal. Biochem.* **1976**, *70*, 495–498. [CrossRef]
9. Nakamura, H.; Takagi, K.; Tamura, Z.; Yoda, R.; Yamamoto, Y. Stepwise fluorometric determination of primary and secondary amines by liquid chromatography after derivatization with 2 methoxy 2,4-diphenyl 3(2H)-furanone. *Anal. Chem.* **1984**, *56*, 919–922. [CrossRef]
10. Bodhe, A.M.; Vartak, H.G.; Rele, M.V.; Dhamankar, V.S. Location and purification of enzymes on polyacrylamide gels using dialyzable fluorescent markers. *Anal. Biochem.* **1987**, *164*, 39–43. [CrossRef]
11. Miedel, M.C.; Hulmes, J.D.; Pan, Y.C. The use of fluorescamine as a detection reagent in protein microcharacterization. *J. Biochem. Biophys. Meth.* **1989**, *18*, 37–52. [CrossRef] [PubMed]
12. Zhu, R.; Kok, W.T. Postcolumn derivatization of peptides with fluorescamine in capillary electrophoresis. *J. Chromatogr. A* **1998**, *814*, 213–221. [CrossRef] [PubMed]
13. Weigele, M.; De Bernardo, S.L.; Leimgruber, W.; Cleeland, R.; Grunberg, E. Fluorescent labeling of proteins. A new methodology. *Biochem. Biophys. Res. Commun.* **1973**, *54*, 899–906. [CrossRef] [PubMed]
14. Tu, S.I.; Grosso, L. Fluorescent labeling of proteins in sodium dodecyl sulfate complexes with fluorescamine. *Biochem. Biophys. Res. Commun.* **1976**, *72*, 9–14. [CrossRef] [PubMed]
15. Barger, B.O.; White, F.C.; Pace, J.L.; Kemper, D.L.; Ragland, W.L. Estimation of molecular weight by polyacrylamide gel electrophoresis using heat stable fluorophors. *Anal. Biochem.* **1976**, *70*, 327–335. [CrossRef] [PubMed]
16. Fishman, M.A.; Hagen, S.; Trotter, J.L.; O'Connell, K.; Agrawal, H.C. Use of a stable fluorescent reagent, 2-methoxy-2,4-diphenyl-3(2H)-furanone, for the visualization and purification of myelin proteins. *J. Neurochem.* **1979**, *32*, 1077–1083. [CrossRef]
17. Falk, B.W.; Elliott, C. Fluorescent monitoring of proteins during sodium dodecyl sulfate-polyacrylamide gel electrophoresis and Western blotting. *Anal. Biochem.* **1985**, *144*, 537–541. [CrossRef]
18. Jackson, P.; Urwin, V.E.; Mackay, C.D. Rapid imaging, using a cooled charge-coupled-device, of fluorescent two-dimensional polyacrylamide gels produced by labeling proteins in the first-dimensional isoelectric focusing gel with the fluorophore 2-methoxy-2,4-diphenyl-3(2H)furanone. *Electrophoresis* **1988**, *9*, 330–339. [CrossRef]
19. Alba, F.J.; Daban, J.R. Nonenzymatic chemiluminescent detection and quantitation of total protein on Western and slot blots allowing subsequent immunodetection and sequencing. *Electrophoresis* **1997**, *18*, 1960–1966. [CrossRef]
20. Sprinzl, M.; Faulhammer, H.G. Participation of X47-fluorescamine modified E. coli tRNAs in in vitro protein biosynthesis. *Nucleic Acids Res.* **1978**, *5*, 4837–4853. [CrossRef]
21. Kasai, H.; Hayami, H.; Yamaizumi, Z.; Saito, H.; Nishimra, S. Detection and identification of mutagens and carcinogens as their adducts with guanosine derivatives. *Nucleic Acids Res.* **1984**, *12*, 2127–2136. [CrossRef] [PubMed]
22. Hawkes, S.P.; Meehan, T.D.; Bissell, M.J. The use of fluorescamine as a probe for labeling the outer surface of the plasma membrane. *Biochem. Biophys Res. Commun.* **1976**, *68*, 1226–1233. [CrossRef] [PubMed]
23. Cross, J.W.; Briggs, W.R. Labeling of membranes from erythrocytes and corn with fluorescamine. *Biochim. Biophys. Acta* **1977**, *471*, 67–77. [CrossRef] [PubMed]
24. Håkanson, R.; Larsson, L.I.; Sundler, F. Fluorescamine: A novel reagent for the histochemical detection of amino groups. *Histochemistry* **1974**, *39*, 15–23. [CrossRef]
25. Larsson, L.I.; Sundler, F.; Håkanson, R. Fluorescamine as a histochemical reagent: Demonstration of polypeptide hormone-secreting cells. *Histochemistry* **1975**, *44*, 245–251. [CrossRef]
26. Bruni, A.; Fasulo, M.P.; Tosi, B.; Dall'Olio, G.; Vannini, G.L. Fluorogenic detection of primary amines in plant histochemistry with fluorescamine: A comparative study on the effects of coagulant and non-coagulant fixatives. *Histochemistry* **1976**, *48*, 269–281. [CrossRef]
27. Sciorra, L.J.; Lee, M.L.; Wynnyckyj, H. Study of human chromosomes. IV. Labeling of chromosomal proteins with the amino group specific fluorescent reagent fluorescamine. *J. Histochem. Cytochem.* **1985**, *33*, 1252–1255. [CrossRef]
28. Cuéllar, T.; Gosálvez, J.; Del Castillo, P.; Stockert, J.C. Fluram induces species-dependent C and G bands in mammalian chromosomes, revealing heterogeneous distribution of chromosomal proteins. *Genome* **1991**, *34*, 772–776. [CrossRef]
29. Stockert, J.C.; Trigoso, C.I. Fluorescence of eosinophil leukocyte granules induced by the fluorogenic reagent 2 methoxy 2,4-diphenyl 3(2H)-furanone. *Blood Cells* **1993**, *19*, 423–430.
30. Sundler, F.; Uddman, R.; Larsson, L.I.; Telenius-Berg, M.; Berg, B.; Håkanson, R. Fluorescamine in diagnosis of thyroid carcinomas. *Acta Cytol.* **1978**, *22*, 54–56.
31. Uddman, R.; Larsson, L.I.; Sundler, F. Fluorescamine as a cytochemical detection reagent for mammary carcinoma cells. *Acta Cytol.* **1978**, *22*, 273–275.
32. Lorch-Jorgensen, L.; Ingemansson, S.; Larsson, L.I. Formaldehyde-fluorescamine-induced fluorescence as a property of carcinoma cells. *Virchows Arch. B Cell Pathol.* **1979**, *30*, 125–130. [CrossRef] [PubMed]

33. Parry, G.; Blenis, J.; Hawkes, S.P. Detection of transformed cells using a fluorescent probe: The molecular basis for the differential reaction of fluorescamine with normal and transformed cells. *Cytometry* **1982**, *3*, 97–103. [CrossRef] [PubMed]
34. De Bernardo, S.; Weigele, M.; Toome, V.; Manhart, K.; Leimgruber, W.; Böhlen, P.; Stein, S.; Udenfriend, S. Studies on the reaction of fluorescamine with primary amines. *Arch. Biochem. Biophys.* **1974**, *163*, 390–399. [CrossRef] [PubMed]
35. Weigele, M.; Tengi, J.P.; De Bernardo, S.; Czajkowski, R.; Leimgruber, W. Fluorometric reagents for primary amines. Synthesis of 2-alkoxy- and 2-acyloxy-3(2H)-furanones. *J. Org. Chem.* **1976**, *41*, 388–389. [CrossRef]
36. Stockert, J.C.; Blázquez-Castro, A. *Fluorescence Microscopy in Life Sciences*; Bentham Science Publishers: Sharjah, United Arab Emirates, 2017. [CrossRef]
37. Stockert, J.C. Reactive staining reagents and fluorescent labels. In *Conn's Biological Stains. A Handbook of Dyes, Stains and Fluorochromes for Use in Biology and Medicine*, 10th ed.; Horobin, R.W., Kiernan, J.A., Eds.; Bios Scientific Publishers: Oxford, UK, 2002; pp. 77–88. ISBN 859960995.
38. Stockert, J.C.; Blázquez, A.; Galaz, S.; Juarranz, A. A mechanism for the fluorogenic reaction of amino groups with fluorescamine and 2 methoxy 2,4-diphenyl 3(2H)-furanone. *Acta Histochem.* **2008**, *110*, 333–340. [CrossRef] [PubMed]
39. Stockert, J.C.; Abasolo, M.I. Inaccurate chemical structure of dyes and fluorochromes found in the literature can be problematic for teaching and research. *Biotech. Histochem.* **2011**, *86*, 52–60. [CrossRef]
40. Stockert, J.C.; Romero, S.A.; Felix-Pozzi, M.N.; Blázquez-Castro, A. In Vitro polymerization of the dopamine-borate melanin precursor: A proof-of-concept regarding 10boron neutron-capture therapy for melanoma. *Biocell* **2023**, *47*, 919–928. [CrossRef]
41. Molero, M.L.; Hazen, M.J.; Pérez Gorroño, A.I.; Stockert, J.C. Simple ß-carboline alkaloids as nucleic acids fluorochromes. *Acta Histochem.* **1995**, *97*, 165–173. [CrossRef]
42. Stockert, J.C.; Cañete, M.; Villanueva, A.; Juarranz, A.; Trigoso, C.I.; Braña, M.F. Fluorescence of chromatin DNA induced by antitumoral naphthalimides. *Z. Nat.* **1997**, *52*, 408–411. [CrossRef]
43. Juarranz, A.; Villanueva, A.; Cañete, M.; Polo, S.; Domínguez, V.; Stockert, J.C. Microscopical and spectroscopic studies on the fluorescence of a daunomycin-aluminum complex. *Histochem. J.* **1999**, *31*, 201–207. [CrossRef] [PubMed]
44. Stockert, J.C.; Del Castillo, P.; Llorente, A.R.; Rasskin, D.M.; Romero, J.B.; Gómez, A. New fluorescence reactions in DNA cytochemistry. 1. Microscopic and spectroscopic studies on nonrigid fluorochromes. *Anal. Quant. Cytol. Histol.* **1990**, *12*, 1–10. [PubMed]
45. Stockert, J.C.; Trigoso, C.I.; Cuéllar, T.; Bella, J.L.; Lisanti, J.L. A new fluorescence reaction in DNA cytochemistry: Microscopic and spectroscopic studies on the aromatic diamidino compound M&B 938. *J. Histochem. Cytochem.* **1997**, *45*, 97–105. [PubMed]
46. Stockert, J.C.; Del Castillo, P.; Romero, J.B.; Tato, A.; Llorente, A.R.; Ferrer, J.M. Orientation of nucleosomes in the 30 nm chromatin fiber as revealed by microscopic studies of linear dichroism and polarized fluorescence. *Biol. Zentralbl.* **1990**, *109*, 471–480.
47. Mello, M.L.S.; Vidal, B.C. Polarization microscopy of extended chromatin fibers. *Meth. Mol. Biol.* **2014**, *1094*, 71–78. [CrossRef]
48. Stockert, J.C. Monomerizing effect of caffeine, o-phenanthroline and tannin on cationic dyes: A model system to analyze spectral characteristics of the intercalative binding to nucleic acids. *Acta Histochem.* **1989**, *87*, 33–42. [CrossRef]
49. Trigoso, C.I.; Del Castillo, P.; Stockert, J.C. Influence of inorganic salts on the staining reaction of eosinophil lecocyte granules by anionic dyes. *Acta Histochem.* **1992**, *93*, 313–318. [CrossRef]
50. Stockert, J.C. The horse eosinophil as a model leucocyte for morphological and cytochemical studies. *Braz. J. Morphol. Sci.* **2005**, *22*, 73–84.
51. Del Castillo, P.; Horobin, R.W.; Blázquez-Castro, A.; Stockert, J.C. Binding of cationic dyes to DNA: Distinguishing intercalation and groove binding mechanisms using simple experimental and numerical models. *Biotech. Histochem.* **2010**, *85*, 247–256. [CrossRef]
52. Stockert, J.C.; Espada, J.; Blázquez-Castro, A. Melanin-binding colorants: Updating molecular modeling, staining and labeling mechanisms, and biomedical perspectives. *Colorants* **2022**, *1*, 91–120. [CrossRef]
53. Stockert, J.C. Molecular modeling of phenyl-boronic acids and catechol-borate esters: A mechanistic rationale for boron binding to melanin catechols, regarding the 10boron neutron-capture therapy of melanoma. *Ann. Rev. Res.* **2022**, *8*, 555726. [CrossRef]
54. Stockert, J.C.; Blázquez-Castro, A.; Horobin, R.W. Identifying different types of chromatin using Giemsa staining. *Meth. Mol. Biol.* **2014**, *1094*, 25–38.
55. Stockert, J.C. Cytochemistry of nucleic acids: Binding mechanism of dyes and fluorochromes. *Biocell* **1985**, *9*, 89–131.
56. Blackburn, G.M.; Gait, M.J. (Eds.) *Nucleic Acids in Chemistry and Biology*; IRL Press: Oxford, UK; New York, NY, USA, 1990; pp. 313–326.
57. Mason, S.F. *Color and the Electronic States of Organic Molecules. Chemistry of the Synthetic Dyes*; J. Wiley and Sons: New York, NY, USA, 1970; pp. 169–221.
58. Stockert, J.C. Lipid peroxidation assay using BODIPY-phenylbutadiene probes: A methodological overview. *Meth. Mol. Biol.* **2021**, *2202*, 199–214. [CrossRef]
59. Stockert, J.C.; Pinna-Senn, E.; Bella, J.L.; Lisanti, J.A. DNA-binding fluorochromes: Correlation between C-banding of mouse metaphase chromosomes and hydrogen bonding to adenine-thymine base pairs. *Acta Histochem.* **2005**, *106*, 413–420. [CrossRef] [PubMed]
60. Horobin, R.W.; Kiernan, J.A. *Conn's Biological Stains. A Handbook of Dyes, Stains and Fluorochromes for Use in Biology and Medicine*, 10th ed.; Bios Scientific Publishers: Oxford, UK, 2002; ISBN 859960995.
61. Moutschen, J.; Degraeve, N.; Moutschen-Dahmen, M. Chromosome fluorescence with berberine. *Cytobiologie* **1973**, *8*, 112–117.

62. Cañete, M.; Villanueva, A.; Juarranz, A.; Stockert, J.C. A study of interaction of thioflavine T with DNA: Evidence for intercalation. *Cell. Mol. Biol.* **1987**, *33*, 191–199.
63. Stockert, J.C.; Trigoso, C.I.; Llorente, A.R.; Del Castillo, P. DNA fluorescence induced by polymethine cation pyrvinium binding. *Histochem. J.* **1991**, *23*, 548–552. [CrossRef]
64. Glazer, A.N.; Rye, H.S. Stable dye-DNA intercalation complexes as reagents for high-sensitivity fluorescence detection. *Nature* **1992**, *359*, 859–861. [CrossRef]
65. Stockert, J.C. 2,5-bis(4-aminophenyl)-1,3,4-oxadiazol: Fluorescence reaction of chromatin and basophilic cytoplasm. *Acta Histochem. Cytochem.* **1983**, *16*, 66–69. [CrossRef]
66. Stockert, J.C.; Pelling, C.; Espada, J. New cationic fluorochromes from diaryloxazole scintillators: Fluorescence of chromatin DNA induced by N-quaternary POPOP derivatives. *Acta Histochem.* **1997**, *99*, 195–205. [CrossRef] [PubMed]
67. Pinna-Senn, E.; Lisanti, J.A.; Ortiz, M.I.; Dalmasso, G.; Bella, J.L.; Gosálvez, J.; Stockert, J.C. Specific heterochromatic banding of metaphase chromosomes using Nuclear Yellow. *Biotech. Histochem.* **2000**, *75*, 132–140. [CrossRef] [PubMed]
68. Stockert, J.C.; Del Castillo, P. Linear dichroism and polarized fluorescence of dye- complexed DNA fibers. *Histochemistry* **1989**, *91*, 263–264. [CrossRef]
69. Saitoh, Y.; Laemmli, U.K. Metaphase chromosome structure: Bands arise from a differential folding path of the highly AT-rich scaffold. *Cell* **1994**, *76*, 609–622. [CrossRef]
70. Weisblum, B.; De Haseth, P.L. Quinacrine, a chromosome stain specific for deoxyadenylate-deoxythymidylate rich regions in DNA. *Proc. Natl. Acad. Sci. USA* **1972**, *69*, 629–632. [CrossRef] [PubMed]
71. Korenberg, J.R.; Engels, W.R. Base ratio DNA content and quinacrine brightness of human chromosomes. *Proc. Nat. Acad. Sci. USA* **1978**, *75*, 3382–3386. [CrossRef]
72. Ferrucci, L.; Mezzanotte, R. A cytological approach to the role of guanine in determining quinacrine fluorescence response in eukaryotic chromosomes. *J. Histochem. Cytochem.* **1982**, *30*, 1289–1292. [CrossRef] [PubMed]
73. Bickmore, W.; Craig, J. *Chromosome Bands: Patterns in the Genome*; Springer: New York, NY, USA, 1997.
74. Diekmann, S.; Zarling, D.A. Unique poly(dA) poly(dT) B′-conformation in cellular and synthetic DNAs. *Nucleic Acids Res.* **1987**, *15*, 6063–6074. [CrossRef]
75. Diekmann, S. DNA curvature. *Nucleic Acids Mol. Biol.* **1987**, *1*, 138–156.
76. Hörz, W.; Altenburger, W. Nucleotide sequence of mouse satellite DNA. *Nucleic Acids Res.* **1981**, *9*, 683–696. [CrossRef]
77. Redi, C.A.; Garagna, S.; Della Valle, G.; Bottiroli, G.; Dell'Orto, P.; Viale, G.; Peverali, F.A.; Raimondi, E.; Forejt, J. Differences in the organization and chromosomal allocation of satellite DNA between the European long tailed house mice *Mus domesticus* and *Mus musculus*. *Chromosoma* **1990**, *99*, 11–17. [CrossRef] [PubMed]
78. Saenger, W. *Principles of Nucleic Acid Structure*; Springer-Verlag: New York, NY, USA; Berlin, Germany, 1984; pp. 385–404.
79. Assa-Munt, N.; Denny, W.A.; Leupin, W.; Kearns, R.D. Proton NMR study of the binding of bis(acridines) to $d(AT)_5 \cdot d(AT)_5$. 1. Mode of binding. *Biochemistry* **1985**, *24*, 1441–1449. [CrossRef] [PubMed]
80. Tekola, P.; Baak, J.P.; Beliën, J.A.; Brugghe, J. Highly sensitive, specific, and stable new fluorescent DNA stains for confocal laser microscopy and image processing of normal paraffin sections. *Cytometry* **1994**, *17*, 191–195. [CrossRef] [PubMed]
81. Ploeger, L.; Dullens, H.F.J.; Huisman, A.; van Diest, P.J. Fluorescent stains for quantification of DNA by confocal laser scanning microscopy in 3-D. *Biotech. Histochem.* **2008**, *83*, 63–69. [CrossRef]
82. Nygren, J.; Svanvik, N.; Kubista, M. The interactions between the fluorescent dye thiazole orange and DNA. *Biopolymers* **1998**, *46*, 39–51. [CrossRef]
83. Prodhomme, S.; Demaret, J.P.; Vinogradov, S.; Asseline, U.; Morin-Allory, L.; Vigny, P. A theoretical and experimental study of two thiazole orange derivatives with single- and double-stranded oligonucleotides, polydeoxyribonucleotides and DNA. *J. Photochem. Photobiol. B Biol.* **1999**, *53*, 60–69. [CrossRef]
84. Hendry, L.B.; Mahesh, V.B.; Edwin, D.; Bransome, E.D.; Ewing, D.E. Small molecule intercalation with double stranded DNA: Implications for normal gene regulation and for predicting the biological efficacy and genotoxicity of drugs and other chemicals. *Mutat. Res.* **2007**, *623*, 53–71. [CrossRef]
85. Shang, X.F.; Morris-Natschke, S.L.; Liu, Y.Q.; Guo, X.; Xu, X.S.; Goto, M.; Li, J.C.; Yang, G.Z.; Lee, K.H. Biologically active quinoline and quinazoline alkaloids. Part I. *Med. Res. Rev.* **2018**, *38*, 775–828. [CrossRef]
86. Ughetto, G.; Wang, A.H.; Quigley, G.J.; van der Marel, G.A.; van Boom, J.H.; Rich, A. A comparison of the structure of echinomycin and triostin A complexed to a DNA fragment. *Nucleic Acids Res.* **1985**, *13*, 2305–2323. [CrossRef]
87. Lown, J.W.; Hanstock, C.C. Structure and function of the antitumor antibiotic carzinophilin A: The first natural intercalative bisalkylator. *J. Am. Chem. Soc.* **1982**, *104*, 3213–3214. [CrossRef]
88. Huang, C.H.; Mong, S.; Crooke, S.T. Interactions of a new antitumor antibiotic BBM-928A with deoxyribonucleic acid. Bifunctional intercalative binding studied by fluorometry and viscometry. *Biochemistry* **1980**, *19*, 5537–5542. [CrossRef] [PubMed]
89. Huang, C.H.; Mirabelli, C.K.; Mong, S.; Crooke, S.T. Intermolecular cross-linking of DNA through bifunctional intercalation of an antitumor antibiotic, luzopeptin A (BBM-928A). *Cancer Res.* **1983**, *43*, 2718–2724. [PubMed]
90. Dai, J.; Punchihewa, C.; Mistry, P.; Ooi, A.T.; Yang, D. Novel DNA bis-intercalation by MLN944, a potent clinical bisphenazine anticancer drug. *J. Biol. Chem.* **2004**, *279*, 46096–46103. [CrossRef] [PubMed]
91. Jobson, A.G.; Willmore, E.; Tilby, M.J.; Mistry, P.; Charlton, P.; Austin, C.A. Effect of phenazine compounds XR11576 and XR5944 on DNA topoisomerases. *Cancer Chemother. Pharmacol.* **2009**, *63*, 889–901. [CrossRef] [PubMed]

92. Lin, C.; Mathad, R.L.; Shang, Z.; Sidell, N.; Yang, D. Solution structure of a 2:1 complex of anticancer drug XR5944 with TFF1 estrogen response element: Insights into DNA recognition by a bis-intercalator. *Nucleic Acids Res.* **2014**, *42*, 6012–6024. [CrossRef]
93. Moorthy, N.S.H.N.; Pratheepa, V.; Ramos, M.J.; Vasconcelos, V.; Fernandes, P.A. Fused aryl-phenazines: Scaffold for the development of bioactive molecules. *Curr. Drug Targets* **2014**, *15*, 681–688. [CrossRef]
94. Antony, S.; Agama, Z.; Miao, K.K.; Hollingshead, M.; Holbeck, S.L.; Wright, M.H.; Varticovski, L.; Nagarajan, M.; Morrell, A.; Cushman, M.; et al. Bisindenoisoquinoline bis-1,3-{(5,6-dihydro-5,11-diketo-11H-indeno[1,2-c]isoquinoline)-6-propylamino}propane bis(trifluoroacetate) (NSC 727357), a DNA intercalator and topoisomerase inhibitor with antitumor activity. *Mol. Pharmacol.* **2006**, *70*, 1109–1120. [CrossRef]
95. Gao, Q.; Williams, L.D.; Egli, M.; Rabinovich, D.; Chen, L.; Quigley, G.J.; Rich, A. Drug-induced DNA repair: X-ray structure of a DNA ditercalinium complex. *Proc. Natl. Acad. Sci. USA* **1991**, *88*, 2422–2426. [CrossRef]
96. Braña, M.F.; Castellano, J.-M.; Morán, M.; Pérez de Vega, M.J.; Romerdahl, C.R.; Qian, X.D.; Bousquet, P.; Emling, F.; Schlick, E.; Keilhauer, G. Bis-naphthalimides: A new class of antitumor agents. *Anticancer Drug Des.* **1993**, *8*, 257–268.
97. Wainwright, M. The use of dyes in modern biomedicine. *Biotech. Histochem.* **2003**, *78*, 147–155. [CrossRef]
98. Feughelman, M.; Langridge, R.; Seeds, W.E.; Stokes, A.R.; Wilson, H.R.; Hooper, C.W.; Wilkins, M.H.F.; Barclay, R.K.; Hamilton, L.D. Molecular structure of deoxyribose nucleic acid and nucleoprotein. *Nature* **1955**, *175*, 834–838. [CrossRef] [PubMed]
99. De Santis, P.; Forni, E.; Rizzo, R. Conformational analysis of DNA-basic polypeptide complexes: Possible models of nucleoprotamines and nucleohistones. *Biopolymers* **1974**, *13*, 3113–3326. [CrossRef] [PubMed]
100. Suau, P.; Subirana, J.A. X-ray diffraction studies of nucleoprotamine structure. *J. Mol. Biol.* **1977**, *117*, 909–926. [CrossRef] [PubMed]
101. Warrant, R.W.; Kim, S.H. α-Helix-double helix interaction shown in the structure of a protamine-transfer RNA complex and a nucleoprotamine model. *Nature* **1978**, *271*, 130–135. [CrossRef] [PubMed]
102. Fita, I.; Campos, J.L.; Puigjaner, L.C.; Subirana, J.A. X-ray diffraction study of DNA complexes with arginine peptides and their relation to nucleoprotamine structure. *J. Mol. Biol.* **1983**, *167*, 157–177. [CrossRef]
103. Rohs, R.; West, S.M.; Sosinsky, A.; Liu, P.; Mann, R.S.; Honig, B. The role of DNA shape in protein–DNA recognition. *Nature* **2009**, *461*, 1248–1254. [CrossRef]
104. Pullman, B. Electrostatics of polymorphic DNA. *J. Biomol. Struct. Dyn.* **1983**, *1*, 773–794. [CrossRef]
105. Aymami, J.; Coll, M.; Frederick, C.A.; Wang, A.H.J.; Rich, A. The propeller DNA conformation of poly(dA)·poly(dT). *Nucleic Acids Res.* **1989**, *17*, 3229–3245. [CrossRef]

Disclaimer/Publisher's Note: The statements, opinions and data contained in all publications are solely those of the individual author(s) and contributor(s) and not of MDPI and/or the editor(s). MDPI and/or the editor(s) disclaim responsibility for any injury to people or property resulting from any ideas, methods, instructions or products referred to in the content.